

# Development on a high-beam-transparency gridded electron gun based on a carbon nanotube cold cathode

Qingyun Chen, Xuesong Yuan, Xiaotao Xu, Yu Zhang, Matthew T. Cole, Yifan Zu, Zexiang Chen, Yong Yin, Hailong Li, Lin Meng and Yang Yan

**Abstract**—We here report on the development of an improved dual-gridded electron gun based on a carbon nanotube cold cathode that enhances electron beam transparency and reduces grid interception and loss pathways. Compared with microscale tip Spindts, the dual-gridded construction decreases challenges associated with nanomaterial growth, fabrication, and assembly. Our experimental findings show that this dual-gridded CNT electron gun can support anode output currents (cathode emission current) of up to 700 mA, with a beam-transparency of up to ~100% and a compression ratio of 1/19. A beam spot of uniform brightness is obtained and the radius of the beam spot is 1.5 mm. In addition, our studies show that the device can operate at 1/100 duty cycle continuous pulse with a stable current of around 100mA over 100 h.

**Index Terms**— Carbon nanotube (CNT), cold cathode, electron gun, field emission, high-beam-transparency.

## I. INTRODUCTION

ELECTRON-OPTICAL systems are a core technology within almost every vacuum electron radiation source (VERS), though their design and effective integration remains challenging[1-5]. Carbon nanotubes (CNTs) have been proven to function as a near ideal field electron emission (FE) cold cathode source [6-8] due to their room-temperature operation, instantaneous switch-on, ability to support large emission current densities, ease of nanoscale self-assembly, and ever

This work was supported by the National Key Research and Development Program of China (No.2019YFA0210202), National Natural Science Foundation of China (No.61771096), Sichuan Science and Technology Program (No.2021YJ0096) and Fundamental Research Funds for the Central Universities (No. ZYGX2019J012). (Corresponding author: Xuesong Yuan.)

Qingyun Chen, Xuesong Yuan, Xiaotao Xu, Yifan Zu, Yong Yin, Hailong Li, Lin Meng and Yang Yan are members of the Terahertz Science and Technology Key Laboratory of Sichuan Province, School of Electronic Science and Engineering, University of Electronic Science and Technology of China, Chengdu 610054, China (e-mail: [cqy@uestc.edu.cn](mailto:cqy@uestc.edu.cn); [yuanxs@uestc.edu.cn](mailto:yuanxs@uestc.edu.cn)).

Yu Zhang is a member of the State Key Laboratory Optoelectronic Materials and Technologies, Sun Yat-sen University, Guangzhou 510275, China. (e-mail: [stszhyu@mail.sysu.edu.cn](mailto:stszhyu@mail.sysu.edu.cn)).

Matthew T. Cole is a member of the Department of Electronic and Electrical Engineering, University of Bath, Bath BA2 7AY, U.K. (e-mail: [m.t.cole@bath.ac.uk](mailto:m.t.cole@bath.ac.uk)).

Zexiang Chen is with the School of Optoelectronic Science and Engineering, University of Electronic Science and Technology of China, Chengdu 610054, China. (e-mail: [zxchen@uestc.edu.cn](mailto:zxchen@uestc.edu.cn)).

decreasing and increasingly competitive production costs [9-16]. However, several integration challenges continue to restrict the development of carbon nanotube (CNT) cold cathode VERS, such as the effective and scalable integration of CNT based electron emitters into macroscopic devices [17-19].

The small modulator size of gridded electron guns with electrostatic focusing systems offer a little explored solution[20]. Nevertheless, in single grid systems the proportion of the cathode current that is intercepted by the grid can be very high, often in excess of 20-55% [18, 19, 21, 22]. The proportionally large current sank into the grid produces excessive grid heating resulting in exacerbated electro-migration within the grid which contributes towards unwanted grid deformation, which reduces operational longevity, and energy losses within the system. Furthermore, due to the high electric field beneath the grid such sagging can encourage local arc discharge between the cathode and grid which further degrades the devices functional life [21, 23].

In this paper, to overcome these restrictions, we propose a novel dual-gridded CNT electron gun which introduces a shadow grid aligned with the control grid within reasonable engineering tolerances and attached to the cathode surface that shapes the CNT FE from a whole plane into a shadowed array, thereby reducing the proportion of electrons intercepted by the control grid. In this arrangement, an electron beam system has been developed that has a high beam-transparency, uniform current density and high-compression-ratio, which collectively highlights the potential of such new device architectures in the development of emerging CNT cold cathode VERS.

## II. SIMULATION

The developed dual-gridded CNT cold cathode electron gun is depicted in Fig. 1(a). It consists of a cathode base (oxygen-free copper), a CNT electron emitter, a stainless-steel planar shadow grid, a stainless-steel planar control grid, a focusing electrode (oxygen-free copper), an anode (SS304), an ITO (Indium-Tin Oxide) conducting glass and an observation window. The ITO conducting glass was separated from the anode by a ceramic insulation. The CNTs were synthesized directly by chemical vapor deposition [16, 24] on the cathode substrate surface, as shown in Fig 1(b). The shadow grid was attached to the CNT cathode surface. The control grid extracted electrons from the CNTs by developing a local electric field of up to 4V/ $\mu\text{m}$  [18, 25]. The control grid and the shadow grid

were aligned with one another using a light microscope.

The design parameters of the dual-gridded electron gun are given in Table I. To simplify fabrication, in addition to shortening the processing time, the mesh-holes and wire-line widths of the shadow grid were equal to those of the control grid. Our simulations indicate that when the wire-line of grid is fixed, the mesh-hole dominates the electric field distribution at the cathode surface. The electric field distribution is relatively flat in this structure which has been reported in our previous study [13]. The electric field at the cathode surface reaches a maximum when the mesh-hole is 0.6 mm.

TABLE I  
DUAL-GRIDDED ELECTRON GUN DIMENSIONS

Symbol	Quantity	Dimension
$r_c$	Cathode substrate radius	6.50 mm
$h_1$ ( $h_2$ )	Mesh hole of grid	0.60 mm
$w_1$ ( $w_2$ )	Mesh wire of grid	0.10 mm
$t_1$ ( $t_2$ )	Thickness of grid	0.06 mm
$D_{c-g}$	Distance between the two grids	0.40 mm
$D_{c-a}$	Distance between cathode and anode	18.0 mm

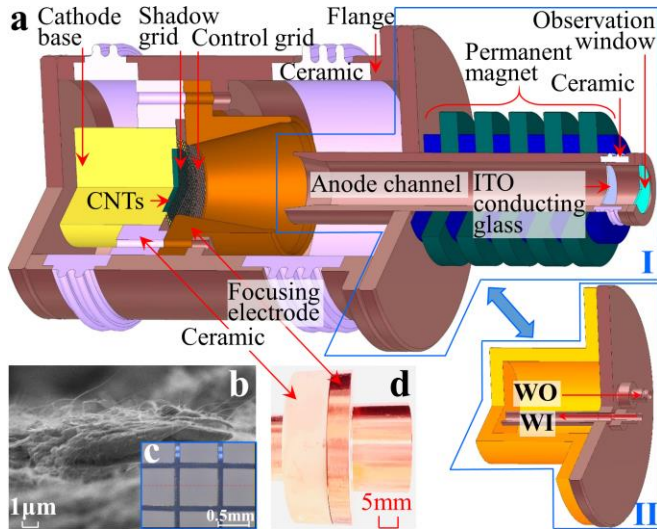


Fig. 1 (a) Scheme of dual-gridded CNT cold cathode electron gun and anode block with water circulation system (II), (WO-water output, WI-water input). (b) Edge-view SEM of an as-grown dense CNT forest thin film on a stainless steel substrate, consisting of CNTs with mean length of 5  $\mu\text{m}$ , as measured elsewhere (Scale bar: 1  $\mu\text{m}$ ) [13], [21]. (c) A typical optical micrograph of the grid (Scale bar: 0.5 mm). (d) Photo of dual-gridded structure with focusing electrode (Scale bar: 5 mm).

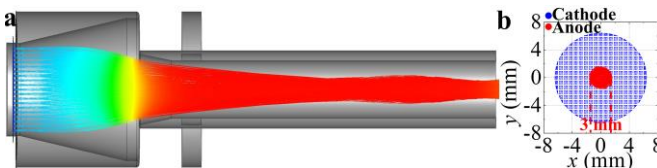


Fig. 2 (a) Simulated beam trajectories within the dual-gridded, CNT-based electron gun. (b) CNT cold cathode emission area and electron beam spot size in the anode plane.

The dual-gridded electron gun has been simulated herein using commercially available 3D particle simulation software. In our simulations the voltages of cathode and shadow grid, control grid, focusing electrode, and anode were set to 0, 4, 4,

and 22 kV, respectively. The emission current from the CNT surface was 500 mA. Analysis of individual electron trajectories suggested that no electron was intercepted by the grid. Fig. 2(b) depicts the simulated beam spot cross-section at the cathode surface and anode output port plane of the electron gun. The electron beam cross-section was compressed from the cold cathode area of  $42.25\pi \text{ mm}^2$  into a beam spot approximately  $2.25\pi \text{ mm}^2$  under the action of an electro-magnetostatic lens. A small-scale permanent magnet (maximum magnetic field 0.13 T) was adopted for this, as shown in Fig.1(a).

### III. EXPERIMENT

Experimentally, the CNT cold-cathode dual-gridded electron gun was sealed in a ceramic and measured in an ultrahigh-vacuum system operated at a base pressure of  $1 \times 10^{-7} \text{ Pa}$ . Measurements were performed using computer-controlled power supply that generates negative voltage pulses with a duration of 100  $\mu\text{s}$  at a repetition frequency of 100 Hz. Triode mode experiments were performed to investigate the beam transparency and the beam focusing.

Here the maximum negative output voltage of power supply was 22 kV. A resistance network was used to provide negative high voltage for the cathode, control grid and anode, as shown in Fig. 3. As the power supply output voltage  $U_s$  increased, the negative high voltage on the cathode and the shadow grid were ramped from 0 to 22 kV. The voltage difference between the cathode and the control grid was 0-5 kV, achieved by adjusting a tunable resistor,  $R_1$ . The ITO conducting glass was connected to earth through a testing resistor,  $R_{\text{test}}$ . The anode was connected to the earth directly. The ITO conducting glass was separated from the anode through ceramic insulation. The anode output current collected on the ITO conducting glass was obtained by testing the voltage on  $R_{\text{test}}$  using an oscilloscope. The cathode emission current and the anode output current were simultaneous measured using the same specification current transformers (CT1 and CT2). The anode output current measured by CT2 (CTS-current transformer signal) and  $R_{\text{test}}$  (TRS-testing resistor signal) were shown to be nominally equivalent to within  $\pm 2\%$  of one another.

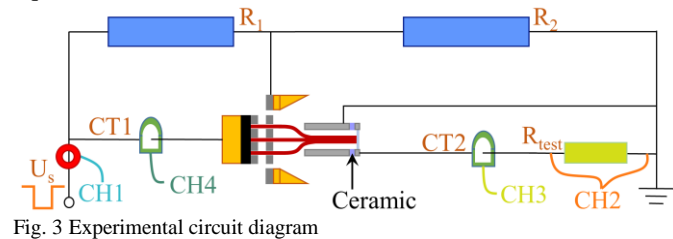


Fig. 3 Experimental circuit diagram

Typical anode current, emission current and high-voltage profiles are shown in Fig. 4(d). The signal amplitudes of the emission current and anode output current were equal and the beam transparency was up to  $\sim 100\%$ . We exchanged CT1 and CT2, and results from the two measurements were identical with each other. Fig. 4(a) shows the anode output current (emission current) as a function of the cathode surface electric field, namely typical  $I$ - $E$  characteristics of the CNT cold

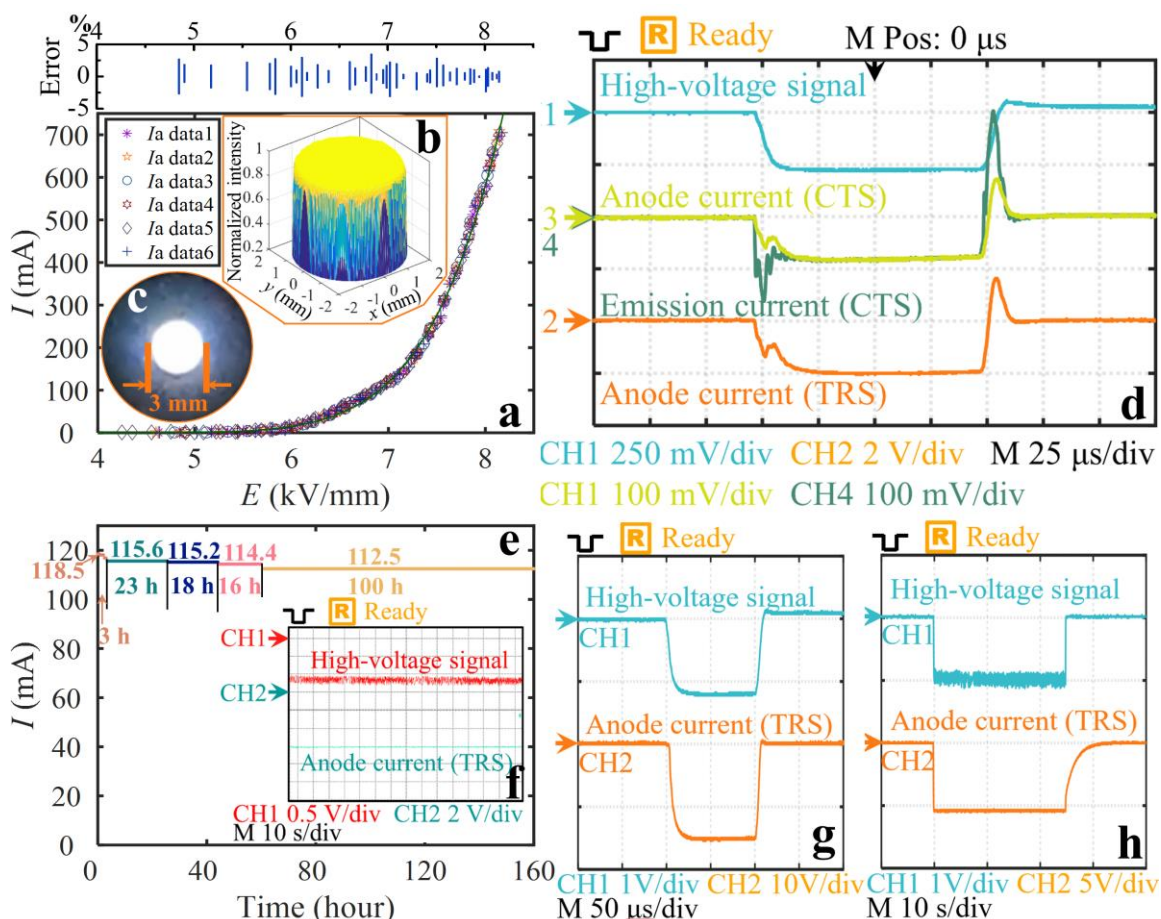


Fig. 4 (a) Typical experimental current ( $I$ )-electric field ( $E$ ) characteristics of the dual-gridded CNT cold-cathode, inset: analysis of measurement error. (b) Brightness distribution along the circle spot. (c) Photo of electron beam spot collected on the ITO conducting glass (Scale bar: 3 mm). (d) Typical temporal switching emission profile of the anode current, emission current and high-voltage signal at 100  $\mu$ s pulse. (e) Emission stability (100  $\mu$ s/100 Hz continuous pulse). Typical profile of the anode current and high-voltage signal at (f) DC mode, (g) 100  $\mu$ s pulse and (h) 25 s pulse.

cathode. The experimental data were obtained after an aging process consisting of a 1% duty cycle continuous pulse for 30 minutes. A fitted emission profile was obtained by applying our fitting produce, as reported elsewhere [15, 17] across the samples and the generalized Fowler-Nordheim equation[26]:  $J=AE^2\exp(-B/E)$ , where  $A$  and  $B$  are  $9.5116 \times 10^{-7} \text{ A/V}^2$  and  $7.3849 \times 10^7 \text{ V/m}$ , respectively ( $R^2 = 0.997$ ). In the triode mode measurements, a maximum anode output current of 700 mA was obtained at an electric field of 8.1kV/mm.

The resulting electron beam spot image, as circled, is shown in Fig. 4(c). The diameter of the nominally circular electron beam was  $\sim 3$  mm. The compression ratio of the electron beam was  $\sim 1/19$  and the operating current density was  $\sim 10\text{A/cm}^2$ , which compares favorably to more complex device structures [19, 21]. The brightness intensity distribution of the measured beam is shown in Fig. 4(b). The brightness uniformity of the circle spot of 96.5% was obtained by the formalism in [24], indicating that the electron beam was extremely uniform on current density according to the luminance signal in the beam spot image.

The emission stability and lifetime of the CNT cold cathode in this new dual-grid structure was measured using an anode block equipped with a water circulation system. In Fig. 1 (a), the anode block with water circulation system (II) replaced the

original anode channel (I) through a CF35 flange. After 160 hours of pulse-mode testing (100  $\mu$ s, 100 Hz), the device showed 118.5 mA/3 h, 115.6 mA/23 h, 115.2 mA/18 h, 114.4mA/16 h, and 112.5 mA/100 h as shown in Fig 4(e). The FE current decreased by only 5% throughout this entire duration. After the short pulse-mode processing, the device operated at long pulse (25 s) with current of 300 mA as shown in Fig. 4(h). Fig. 4(f) shows the device operated at DC mode with a stable current of 75 mA during the testing time of 1 h.

#### IV. CONCLUSION

A dual-gridded CNT cold cathode electron gun with a large anode current has herein been realized, and that has been shown capable of providing beam transparencies  $\sim 100\%$ . Compared with microscale tip Spindt-type structures, the macroscale CNT forest cathodes used here are shaped by the shadow grid removing the need for complex and time-consuming lithographic processing of the CNTs, whilst also providing increased spatial uniformity. The proposed dual-gridded electron gun is simple to fabricate and assemble. The present structure demonstrates the feasibility of dual-gridded CNT cold-cathode electron guns and highlights their potential deployment in millimeter-wave VERS.

## REFERENCES

- [1] J. Sweigle, E. Schamiloglu, and J. Benford, "High Power Microwaves, Second Edition," *High Power Microwaves, Second Edition. Series: Series in Plasma Physics, ISBN: 978-0-7503-0706-2. Taylor & Francis, Edited by John Sweigle, Edl Schamiloglu and James Benford*, 02/01, 2007, doi: 10.1201/9781420012064.
- [2] R. J. Umstatt, D. Abe, J. Benford, D. Gallagher, R. M. Gilgenbach, D. M. Goebel, M. S. Litz, and J. A. Nation, "Cathodes and Electron Guns," *High-Power Microwave Sources and Technologies*, J. B. Robert and S. Edl, eds., pp. 284-324, Piscataway, NJ: Wiley-IEEE Press, 2001.
- [3] C. Abdallah, R. J. Barker, R. M. Gilgenbach, D. M. Goebel, Y. Y. Lau, R. M. Phillips, E. Schamiloglu, and A. Singh, "Beam Transport and RF Control," *High-Power Microwave Sources and Technologies*, J. B. Robert and S. Edl, eds., pp. 250-283, Piscataway, NJ: Wiley-IEEE Press, 2001.
- [4] G. Faillon, G. Kornfeld, E. Bosch, and M. K. Thumm, "Microwave Tubes," *Vacuum Electronics: Components and Devices*, J. A. Eichmeier and M. K. Thumm, eds., pp. 1-84, Berlin, Heidelberg: Springer Berlin Heidelberg, 2008.
- [5] A. S. Gilmour, and I. Ebrary, *Klystrons, traveling wave tubes, magnetrons, crossed-field amplifiers, and gyrotrons*, p.^pp. 21, Fitchburg, USA: Artech House, 2011.
- [6] Y. Di, M. Xiao, X. Zhang, Q. Wang, C. Li, W. Lei, and Y. Cui, "Large and stable emission current from synthesized carbon nanotube/fiber network," *Journal of Applied Physics*, vol. 115, no. 6, pp. 064305, 2014/02/14, 2014, doi: 10.1063/1.4864431.
- [7] W. Lei, X. Zhang, J. Chen, Z. Zhao, Y. Cui, and B. Wang, "Very High Field Emission from a Carbon Nanotube Array With Isolated Subregions and Balanced Resistances," *IEEE Transactions on Electron Devices*, vol. 58, no. 10, pp. 3616-3621, 2011, doi: 10.1109/TED.2011.2162520.
- [8] Q. Wang, C. Yu, Y. Di, Z. Zhu, X. Zhang, C. Li, and W. Lei, "High-Current-Density field emission from self-heating printed carbon nanotubes," *Fullerenes, Nanotubes and Carbon Nanostructures*, vol. 24, no. 4, pp. 273-277, 2016/04/02, 2016, doi: 10.1080/1536383X.2016.1152470.
- [9] A. S. Berdinsky, A. Shaporin, J. B. Yoo, J. Park, P. S. Alegaonkar, J. Han, and G. H. Son, "Field enhancement factor for an array of MWNTs in CNT paste," *Applied Physics A*, vol. 83, pp. 377-383, 01/06, 2006, doi: 10.1007/s00339-006-3482-7.
- [10] D. S. Bethune, C. H. Kiang, M. S. de Vries, G. Gorman, R. Savoy, J. Vazquez, and R. Beyers, "Cobalt-catalysed growth of carbon nanotubes with single-atomic-layer walls," *Nature*, vol. 363, no. 6430, pp. 605-607, 1993/06/01, 1993, doi: 10.1038/363605a0.
- [11] J.-M. Bonard, J.-P. Salvetat, T. Stöckli, W. A. d. Heer, L. Forró and A. Châtelain, "Field emission from single-wall carbon nanotube films," vol. 73, no. 7, pp. 918-920, 1998, doi: 10.1063/1.122037.
- [12] Z. Chen, G. Cao, Q. Zhang, P. Lan, B. Zhu, T. Yu, and Z. Lin, "Large current carbon nanotube emitter growth using nickel as a buffer layer," *Nanotechnology*, vol. 18, no. 9, pp. 095604, 2007/01/24, 2007, doi: 10.1088/0957-4484/18/9/095604.
- [13] Q. Chen, X. Yuan, M. T. Cole, Y. Zhang, L. Meng, and Y. Yan, "Theoretical Study of a 0.22 THz Backward Wave Oscillator Based on a Dual-Gridded, Carbon-Nanotube Cold Cathode," *Applied Sciences-Basel*, vol. 8, no. 12, pp. 2462, 2018, doi: 10.3390/app8122462.
- [14] X. Yuan, Q. Chen, X. Xu, M. T. Cole, Y. Zhang, Z. Chen, and Y. Yan, "A Carbon Nanotube-Based Hundred Watt-Level Ka-Band Backward Wave Oscillator," *IEEE Transactions on Electron Devices*, pp. 1-6, 2021, doi: 10.1109/TED.2021.3066144.
- [15] M. Cole, K. Teo, O. Gröning, L. Gangloff, P. Legagneux, and W. Milne, "Deterministic Cold Cathode Electron Emission from Carbon Nanofibre Arrays," *Scientific reports*, vol. 4, pp. 4840, 05/02, 2014, doi: 10.1038/srep04840.
- [16] M. T. Cole, K. Hou, J. H. Warner, J. S. Barnard, K. Ying, Y. Zhang, C. Li, K. B. K. Teo, and W. I. Milne, "In-situ deposition of sparse vertically aligned carbon nanofibres on catalytically activated stainless steel mesh for field emission applications," *Diamond and Related Materials*, vol. 23, pp. 66-71, 2012/03/01/, 2012, doi: 10.1016/j.diamond.2011.12.039.
- [17] X. Yuan, Y. Zhang, M. Cole, X. Li, R. Parmee, J. Wu, N. Xu, W. Milne, and S. Deng, "A truncated-cone carbon nanotube cold-cathode electron gun," *Carbon*, vol. 120, pp. 374-379, 03/01, 2017, doi: 10.1016/j.carbon.2017.03.046.
- [18] X. Yuan, Y. Zhang, H. Yang, X. Li, N. Xu, and S. Deng, "A Gridded High Compression Ratio Carbon Nanotube Cold Cathode Electron Gun," *IEEE Electron Device Letters*, vol. 36, pp. 1-1, 04/01, 2015, doi: 10.1109/LED.2015.2401593.
- [19] G. Ulisse, C. Ciceroni, F. Brunetti, and A. D. Carlo, "Electrostatic Beam Focusing of Carbon Nanotubes Electron Source," *IEEE Transactions on Electron Devices*, vol. 61, no. 7, pp. 2558-2563, 2014, doi: 10.1109/TED.2014.2324171.
- [20] Y. Di, Q. Wang, X. Zhang, W. Lei, X. Du, and C. Yu, "A vacuum sealed high emission current and transmission efficiency carbon nanotube triode," *AIP Advances*, vol. 6, no. 4, pp. 045114, 2016/04/01, 2016, doi: 10.1063/1.4948263.
- [21] G. Ulisse, F. Brunetti, E. Tamburri, S. Orlanducci, M. Cirillo, M. L. Terranova, and A. D. Carlo, "Carbon Nanotube Cathodes for Electron Gun," *IEEE Electron Device Letters*, vol. 34, no. 5, pp. 698-700, 2013, doi: 10.1109/LED.2013.2250247.
- [22] W. Knapp, and D. Schleußner, "Special features of electron sources with CNT field emitter and micro grid," *Applied Surface Science*, vol. 251, no. 1, pp. 164-169, 2005/09/15/, 2005, doi: 10.1016/j.apsusc.2005.03.200.
- [23] Y. S. Di, Q. L. Wang, X. B. Zhang, W. Lei, X. F. Du, and C. R. Yu, "A vacuum sealed high emission current and transmission efficiency carbon nanotube triode," *Aip Advances*, vol. 6, no. 4, Apr, 2016, doi: 10.1063/1.4948263.
- [24] X. Yuan, W. Zhu, Y. Zhang, N. Xu, J. Wu, Y. Shen, J. Chen, J. She, and S. Deng, "A Fully-Sealed Carbon-Nanotube Cold-Cathode Terahertz Gyrotron," *Scientific Reports*, vol. 6, pp. 32936, 09/09, 2016, doi: 10.1038/srep32936.
- [25] N. Bushuev, Y. Grigoriev, A. Bourtsev, P. Schalaev, and E. Tarasov, "Multibeam electron gun with gated carbon nanotube cathode." pp. 559-560.
- [26] L. W. Nordhiem, and R. H. Fowler, "The effect of the image force on the emission and reflexion of electrons by metals," *Proceedings of the Royal Society A Mathematical Physical & Engineering Sciences*, vol. 121, no. 788, pp. 626-639, 1928, doi: doi:10.1098/rspa.1928.0222.